International Journal of Mechanical Sciences 178 (2020) 105588

Contents lists available at ScienceDirect

International Journal of Mechanical Sciences

journal homepage: www.elsevier.com/locate/ijmecsci

Hardening vs. softening dichotomy of a hinged-simply supported beam with one end axial linear spring: Experimental and numerical studies

Lukasz Kloda[a,b,*], Stefano Lenci[a], Jerzy Warminski[b]

[a] Department of Civil and Building Engineering, and Architecture, Polytechnic University of Marche, via Brecce Bianche, Ancona 60131, Italy
[b] Department of Applied Mechanics, Lublin University of Technology ul. Nadbystrzycka, Lublin 36 20-618, Poland

ARTICLE INFO

Keywords:
Kinematically excited vibrations
Nonlinear damping
Identification tests
Finite element method

ABSTRACT

The aim of this paper is to validate experimentally a nonlinear model of a kinematically excited hinged-simply supported beam with a spring subjected to one end. An experimental setup configuration enables to test different variants of axial boundary conditions: first a typical simply supported beam (no spring), and next two different spring systems. The prototype is kinematically excited with different amplitudes of excitation and then full frequency response curves are drawn wherein hardening/softening dichotomy is recognized. A set of mechanical properties of the system is identified and then used to reproduce tests with finite element simulations. Consequently numerical vs. experiment results are compared. The analysis demonstrates amplitude dependent damping as well as that the natural frequency depends on environmental conditions, and thus may change over experiments.

1. Introduction

Beams are deformable structural elements used in civil, electrical, mechanical, ocean and space engineering due to their capacity of carrying payloads, compound complex structures, or being a main working part of sensors. Simultaneously they are one of the basic element of theoretical interest in applied mechanics and are modeled in numerous ways. The essential difference in the beam response may be observed if the model is nonlinear [1–4]. Recent advances in computational power allows us to introduce sophisticated mechanical effects, compute the systems with higher order nonlinearities and consequently realize a solution of higher accuracy [5–7]. Discrepancies between a real structure and theoretical models may be also due to some approximations in the description of real boundary conditions (BCs). In fact, BCs are commonly assumed to ideal, i.e. they exact eliminate the corresponding displacement, while in practice they often have a stiffness allowing some, minor, movements. As presented in [8–11], properly describing the behaviour of BCs can be essential for response of the whole system.

Studies on hinged-simply-supported and hinged-hinged beams are motivated by the occurrence of hardening/softening phenomena and bifurcation of solutions existing for large amplitudes of oscillations together with strong nonlinearity of the system [12,13]. Furthermore, an intermediate case of the simply-supported and hinged-hinged beams can be considered by applying a boundary spring in the axial direction, so that we can continuously go from simply-supported (axially movable) to hinged (axially immovable) cases by increasing from 0 to ∞ the stiffness of the spring (see Fig. 1). As a matter of fact, by modifying spring stiffness the dynamical response of the structure changes from softening to hardening. This phenomenon can be used for passive control of the beam dynamics [14].

The planar hinged-simply supported beam model with axial spring at one end was derived in [15,16]. The geometrical nonlinearities were taken into account in the model. Apart from the longitudinal, transversal and rotational inertia, the geometric nonlinear curvature included also shearable rotation of a beam cross-section. A lot of attention was paid to development of that model on free [17–19] and forced-damped oscillations [20–23], where various perturbation techniques and finite element methods were used.

In general, the analytical and numerical methods were in excellent agreement close to resonant frequencies. Hovewer, in contrast to the analytical solution, the numerical simulations performed in time domain (explicitly) by FE method enable to capture multi-mode response and gives reliable outcomes also even far away from the resonant frequencies. For these reasons we decided to use this method, despite the time-consuming simulation process.

Although, numerical and analytical analysies accurate the final correctness of the results must be confirmed experimentally: *"Experiment is the sole source of truth. It alone can teach us something new; it alone can give us certainty"* [24]. Thus, the main purpose of this work is to supplement the extensive theoretical research on simply supported beams

* Corresponding author at: Department of Applied Mechanics, Lublin University of Technology ul. Nadbystrzycka, 36 20-618 Lublin, Poland.
E-mail address: l.kloda@pollub.pl (L. Kloda).

https://doi.org/10.1016/j.ijmecsci.2020.105588
Received 2 September 2019; Accepted 5 March 2020
Available online 12 March 2020

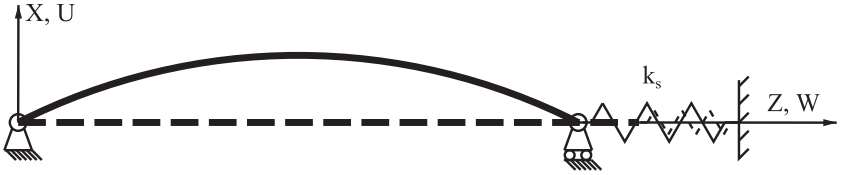

Fig. 1. Simply supported beam with an axial spring.

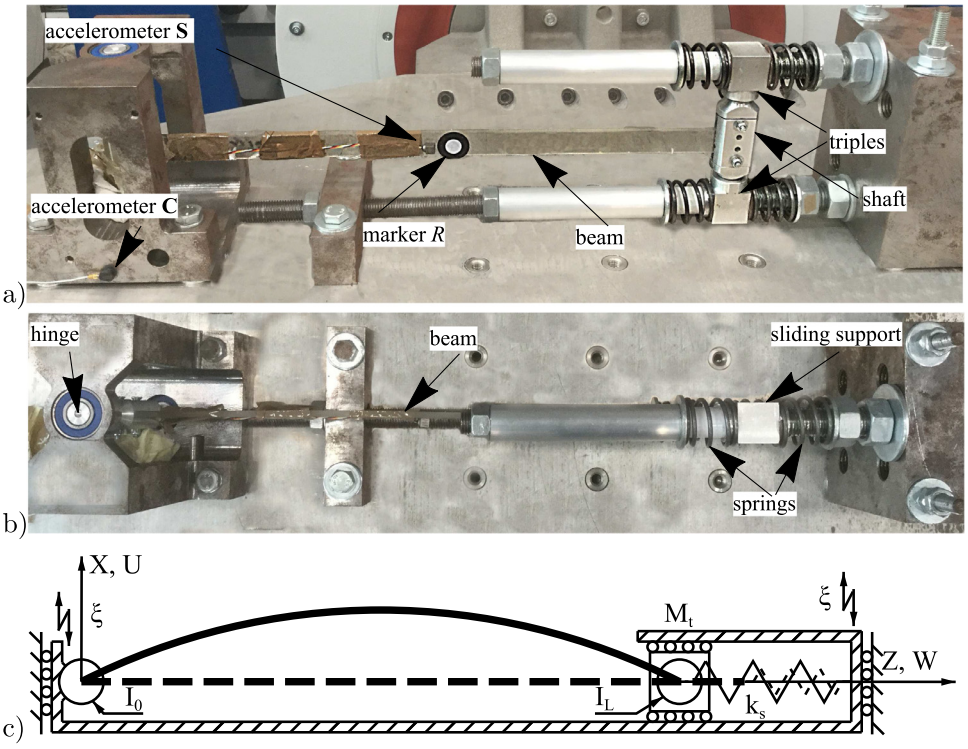

Fig. 2. Beam-spring system mounted on the slip table: front (a) and top (b) views. Schematic representation (top view) of the kinematically excited system with translational and rotatory inertia (c).

with spring boundary conditions [16–22] and carry out the important experimental test, which is aimed to practically demonstrate the change from softening phenomenon (simply supported beam) to hardening behavior (hinged-hinged beam). As it is shown in this paper, research has revealed new phenomena, which need a further development in the future.

The paper is organized as follows. Section 2 describes prototype and identification of the static properties of the beam-spring system; the analysis involves beam material characteristics, effective springs stiffness as well inertia element related to hinges and translational tip mass. Dynamic tests of free oscillations in two different temperatures and full frequency response curves of the kinematically excited system are presented. Next, finite element modeling, static and dynamic analysis as well as of method of fitting frequency response curves are shown in Section 3. Finally, a cross-check of experiments and numerics is performed in Section 4. The paper ends with some conclusions.

2. Experimental test

2.1. Setup

The experimental setup consists of a homogeneous rectangular plexiglass slender beam, bearing shaft on the left hand side, platen coupled with sliding supports through two triples and four springs arranged axially, see Fig. 2a and b. The system is grounded with robust modules to a plane of slip table. Immovable elements are made of steel, while movable parts are designed of aluminum, which limit effect of rotary and translational inertia. Sliding contact surfaces have been covered with thin Teflon sleeves. The system of four push springs is tightened with an appropriate preload, which works in positive and negative directions. The elastic bound can be replaced as well as removed. The beam is mounted to the holder at the last stage of assembly, it prevents pre-stresses of the beam and allows sufficient clamp. In order to avoid bending in two perpendicular directions and reduce the system to a planar problem, the dimensions of the cross-section of the beam are set as in Table 1. To prevent axial-transversal internal resonance, the dimensions of the beam are chosen so that natural frequencies of longitudinal and flexural vibrations are well separated. To represent the real system more adequately, the model in Fig. 1 is modified by additional components presented in Fig. 2c, i.e. we add in the numerical model new masses that may move along the axial direction of the beam (M_t) and rotate in horizontal plane (I_0, I_L). This generates dynamical boundary condition involving additional inertia terms.

2.2. Static properties identification of the beam-spring system

Material properties of the beam are listed in Table 1. Modulus of elasticity is determined on the testing machine, see Fig. 3. In spite of good agreement between strength test and literature [25], the modulus of elasticity is also calculated from the first natural frequency and its corresponding bending mode. This procedure tuned natural frequencies of the prototype and finite element model [26]. We refer Poisson's ratio coefficient to [25]. The density is calculated from beam's volume and mass measured on a precision balance.

The effective stiffness of two pairs of springs in the longitudinal direction has been tested on *Shimatzu AGS-X 5kN* strength machine by compression and extension tests (see Fig. 3a). The beam-specimen was swapped with robust steel bar, axial tensile load is limited by the con-

Table 1
The physical properties and dimensions of the Plexiglas prismatic beam.

Young's modulus	Poison's ratio	Mass density	Length	Width	Height
E	ν	ρ	L	b	h
3.3 GPa	0.35	1245.05 kg/m^3	0.45 m	20 mm	4.75 mm

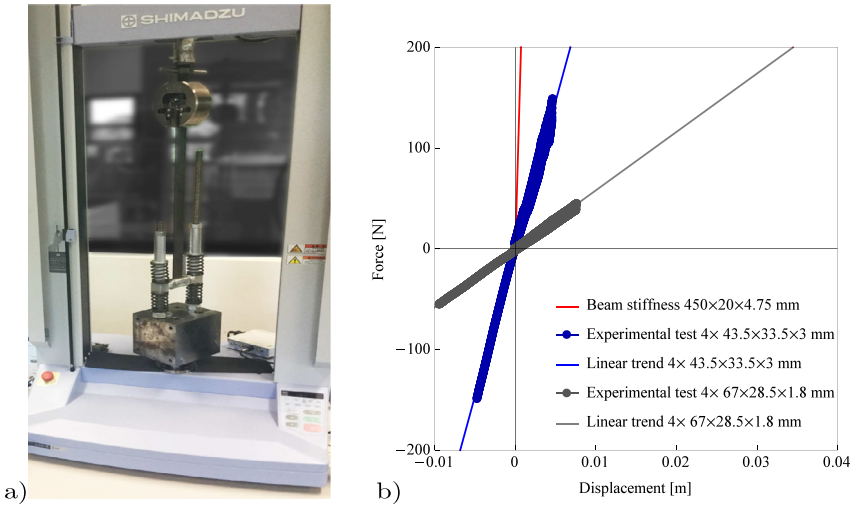

Fig. 3. Spring system stiffness identification: strength test (a) and results (b).

siderable mass of the module (18.3 kg). Relatively slow test's feed rate (50 mm/min) neglects dynamical effects. The suspension composed of four springs 43.5 × 33.5 × 3 mm and 67 × 28.5 × 1.8 mm have linear nature (Fig. 3b) and dummyTXdummy- can be defined by linear stiffness coefficients $k_s = 29254$ N/m and $k_s = 5798.5$ N/m, respectively. The tip mass is $M_t = 0.155$ kg which includes also mass of the shaft and two triples presented in Fig. 2a. The left hinge has mass moment of inertia $I_0 = 1.0928 \times 10^{-5}$ kg m^2 while that on the right, which in mounted on the shaft which is movable along beam's axis is $I_L = 7.556 \times 10^{-6}$ kg m^2. In the forthcoming Section 2.3 more details are presented about the setup prepared for experimental tests.

2.3. Experimental dynamic tests

The laboratory equipment has some physical limitations [27]. The used oil film slip table TGT MO 48 XL enabled to run the shaker and apply frequency of excitation Ω between 15 Hz and 30 Hz and four amplitudes of excitation $\xi = 1$ mm, $\xi = 1.5$ mm, $\xi = 2$ mm and $\xi = 2.5$ mm. The control accelerometer $\boldsymbol{C}$ is placed on the movable table while a three-axial sensor $\boldsymbol{S}$ is fixed to the midpoint of the beam (see Fig. 2a). The frequency of excitation has been swept backward (Ω_-) from 30 Hz to 15 Hz, then chirp sweep forward (Ω_+). Total time of the sweep forward and backward is 308 s, wherein start-up (30 Hz) took 2 s, then sweep backward duration is 150 s and shutdown (15 Hz) lasted 2 s. The process has been repeated in opposite direction, beginning from 2 s of start-up (15 Hz), has been continued by sweep forward by 150 s and one full course ended with 2 s of shutdown (30 Hz). The sweep rate has been set as 0.1 Hz/s. Absolute displacement $E_a(\Omega)$ and its time shift $\varphi(\Omega)$ with respect to controller $\boldsymbol{C}$ have been recorded. In post processing, the experimental relative amplitude ($E_r(\Omega)$) of oscillations with respect to the moving coordinate system preset on the slip plate is calculated as:

$$E_r(\Omega) = E_a(\Omega) + \xi \cos[\varphi(\Omega)] \tag{1}$$

Examples of the frequency response curves are shown in Fig. 4 and full experimental results will be collectively presented in Section 4. Analysis will include four amplitudes of excitation for three types of boundary conditions and sweeps forward/backward for all of them, in total 24 experimental curves. Laboratory results will be compared with precisely matched numerical simulations performed in Section 3.2.

Before developing numerical simulations, system's free vibration tests are also performed in two different room temperatures 23 °C (Fig. 5a) and 28 °C (Fig. 5b). Firstly, the structure has been perturbed and then free oscillations of the reflective marker R (see Fig. 2a) has been recorded with the use of contactless laser scanner vibrometer Polytec PSV-500. Test is repeated four times for the system with spring stiffness $k_s = 29254$ N/m. Time histories show a large difference in the course of natural vibration in both temperatures. We interpret that the structure undergoes a hardening phenomenon. It means that period of oscillations decreases as the maximum amplitude falls dawn. The damping coefficient is lower for higher amplitudes of oscillations as well as in all cases smaller for higher temperature. These preliminary tests are presented to highlight the complexity of the problem. The laboratory temperature grows naturally during the day and the structure is additionally heated by the vibration generator. It is very unlikely to reconstruct a smooth backbone curve because the amplitude of oscillations decreases very fast (5 cm of initial deflection vanish in 5–6 cycles), consequently energy absorption in the system takes place much faster than one full period and the experiment is difficult to repeat in constant environmental conditions. For the above-mentioned reasons, in comparable numerical calculations, the damping factor is adjusted individually for each of the resonance curves [28–30].

3. Finite element analysis

3.1. Beam model

Numerical model is composed of 100, *B21 type* finite elements. B21 is Abaqus_CAE© basic planar beam element that uses linear interpolation between nodes. Additionally, true stress and strain are calculated with use *NLgeom* function, suitable for large amplitudes vibrations [31]. In rest condition, each beam element has equal length and its properties are defined as in Table 1. Kinematic constraints are defined as follows:

$$U(0,T) = U(L,T) = 0, \quad W(0,T) = 0 \tag{2}$$

Leaving the freedom of axial movement and rotation, the additional moment of inertia I_0 and I_L as well as the tip mass M_t are included in the numerical model. The axial spring links the end of the beam and origin

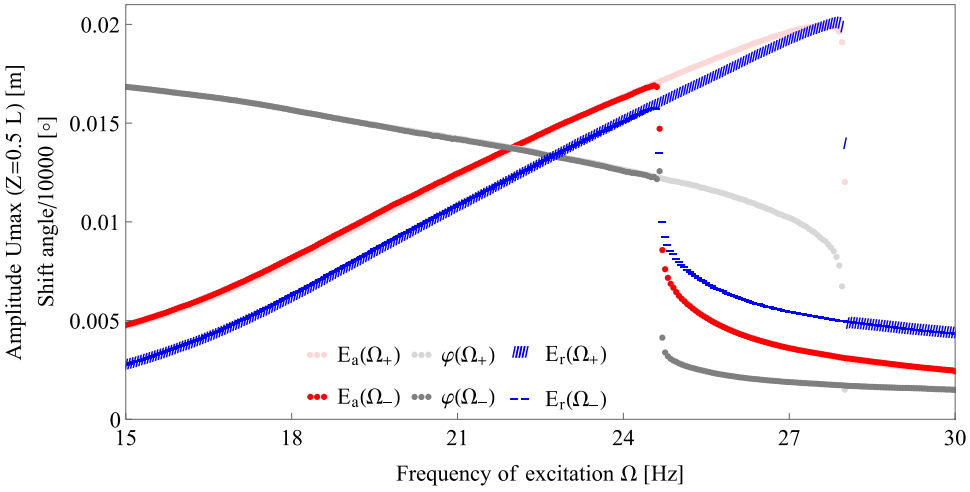

Fig. 4. Absolute frequency response curves $E_a(\Omega_\pm)$ together with shift angle $\varphi(\Omega_\pm)$ and corresponding relative amplitudes $E_r(\Omega_\pm)$; k_s = 29254 N/m, ξ = 1.5 mm.

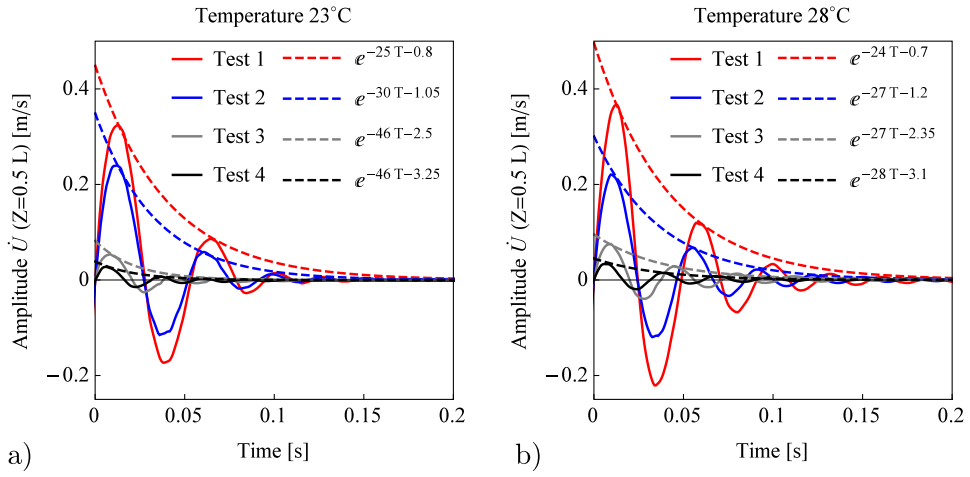

Fig. 5. Free oscillations (solid lines) and matched logarithmic decrements of damping (dashed lines) for the beam-spring system tested in two temperatures.

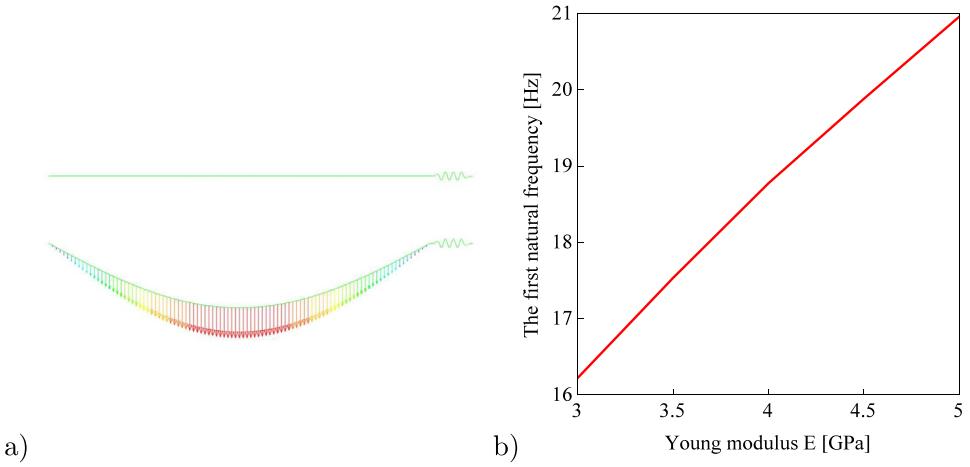

Fig. 6. The numerical model (top) and the analyzed mode shape (bottom) obtained for natural frequency ω_0 = 19.75 Hz (a). The natural frequency of first bending mode related to modulus of elasticity (b). Computations performed in *Linear perturbation, Frequency* module with use of *Lanczos Eigensolver*.

of the local coordinate system (movable with a beam). The FE model displayed in Fig. 6a (top) reflects the setup arrangement shown in Fig. 2c.

Fig. 6 displays undeformed beam and the image of the first natural bending mode resultant deformations. It is worth to remark that natural frequencies and corresponding flexural modes are independent of boundary conditions like sliding mass inertia and spring in axial direction [22], but moment of inertia does affect and cannot be ignored in the model. Both, tip mass and rotatory inertia decreases natural frequencies in longitudinal and transverse directions, respectively. On the other hand, axial spring increases the linear natural frequencies in the longitudinal direction.

3.2. Path following

Investigations in the linear regime are now extended to study nonlinear dynamics of the system. Calculations involve kinematic excitation

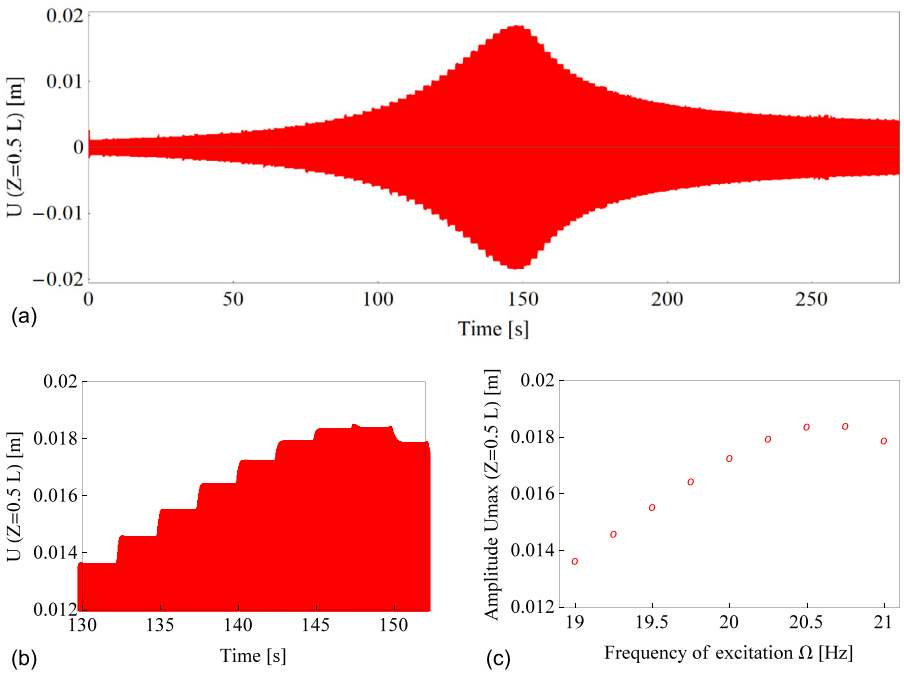

Fig. 7. Post processing method: full time history of relative amplitude (a), selected interval of time signal (b) and its conversion to frequency domain (c); $k_s = 5798.5$ N/m, $\xi = 2.5$ mm, $\zeta = 9$ %.

in the neighborhood of the primary resonance, and boundary conditions (2) accordingly change into

$$U(0,T) = U(L,T) = \xi \cos(\Omega T), \quad W(0,T) = 0. \tag{3}$$

Simulation have been performed in 121 computational steps, wherein each step is responsible for nth frequency of excitation, and the frequency is slightly increased of 0.25 Hz starting at $\Omega = 10$ Hz and finishing at $\Omega = 40$ Hz. Maintaining constant frequency Ω and amplitude ξ of excitation for 50 periods (if necessary 100), the transient oscillations vanish and the motion becomes periodic. The deformation at the end of the simulation ($n = j - 1$) becomes the initial condition for the next frequency ($n = j$). The frequencies jump gradually step by step, creating just a slight disturbance of the system. The time history is presented in Fig. 7a. Recording relative displacements of beam's midpoint, the maximum amplitude $N_r(\Omega_\pm)$ is assigned to the corresponding frequency Ω (which is known from the excitation).

The indicated procedure is presented in Fig. 7b and c. For different values of the damping ζ the frequency response curves $N_r(\Omega_-)$ are drawn in Fig. 8. This approach allows to follow only stable paths, and when stability is lost a jump to another solution or other different phenomena can be detected, as presented in [20]. The considered case does not show any irregular of unexpected behaviour. The maximum amplitude of the frequency response curve is slightly shifted toward the right with respect to $\omega_0 = 19.75$ Hz, showing a weak hardening nature; the jump phenomenon does not occur.

The dynamical analysis includes investigation on the effects of the damping coefficient. In our approach a linear viscous damping is always assumed. For each frequency response curve it is determined by the best fitting between numerical and experimental results. The damping coefficient is crucial in the neighborhood of resonance (18 – 24 Hz), while away it has a minor effect on the results. To match results, which indeed are temperature dependent, the Young modulus is also fitted to tune natural frequency. Changes of natural frequency in experiment are about 0.75 Hz, between 19.25 Hz and 20.00 Hz, therefore in the numerical model the modulus of elasticity is tuned to 4.4 GPa $\pm$ 4 %, see the relation $\omega_0(E)$ presented in Fig. 6b.

4. FEM vs. experiment

The nonlinear response of simply supported beam is constructed on the laboratory prototype. Then identification procedure allowed to get a very good agreement of the FE model with experimental tests for all three cases which demonstrate different behaviors.

Lack of spring generates softening phenomenon, as shown in Fig. 9. In this case the experimental curves have the highest noise ratio, and for constant amplitude of excitation two-way sweep responses are slightly shifted and also small amplitude change appears. This is likely due to the noise observed in the output signal, which is generated by the moving parts. Micro-gaps between those parts generate micro impacts, which are present in the measured signal. Additional set of springs suppresses this effect. The procedure of constructing curves started from the highest amplitude $\xi = 2.5$ mm and then the amplitude was decreased about 0.5 mm up to $\xi = 1$ mm, accordingly to columns in plot label. It is observed that damping ratio ζ decreases as (i) the amplitude of excitation decreases (this is clearly visible in Figs. 9–11) and (ii) when the temperature increases (not reported results). This effect has been confirmed in Fig. 5a and b.

The addition of an axial end spring, even of lower stiffness, generates slight hardening phenomenon (Fig. 10). Quality of the plots is much better, with almost no shifts of forward and backward branches. Again, damping decreases for decreasing amplitudes.

Fig. 11 shows the third case with the spring of higher stiffness, which demonstrates strong hardening. Here hystereses of frequency response curves appear for amplitudes of excitation equal or higher than 1.5 mm. Curves $E_r(\Omega_\pm)$, $\xi = 1.5$ mm are shifted with respect to each other of about 0.5 Hz. It may be caused by rapid change of the length of the beam, which could be a result of combined temperature-preload issues. It is very likely that both effects appear simultaneously.

5. Conclusions

The forced-damped nonlinear dynamics of a beam, hinged at the left side and simply supported at the right side with an axial spring, have been studied experimentally and numerically. Based on identified mechanical properties of the prototype, the FE model of the beam with a linear spring has been created. To match the real structure the rotation

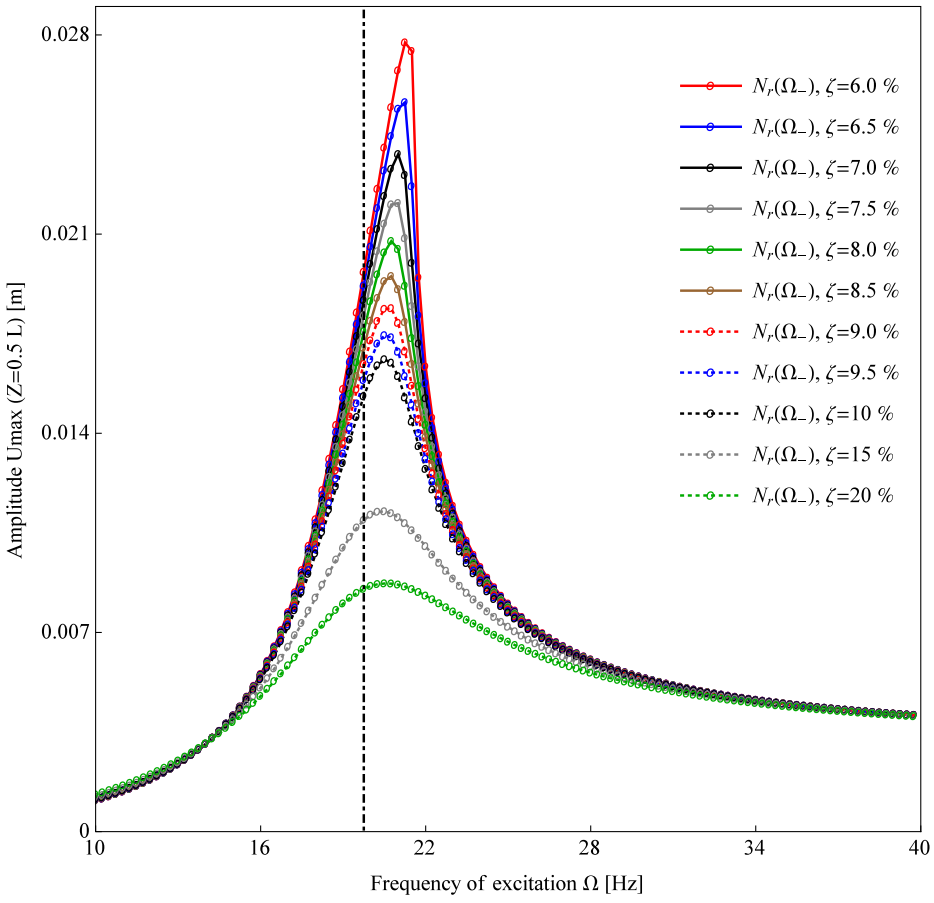

Fig. 8. Frequency response curves FEM: damping test. The black dot-dashed vertical line reflects the natural frequency of the system.

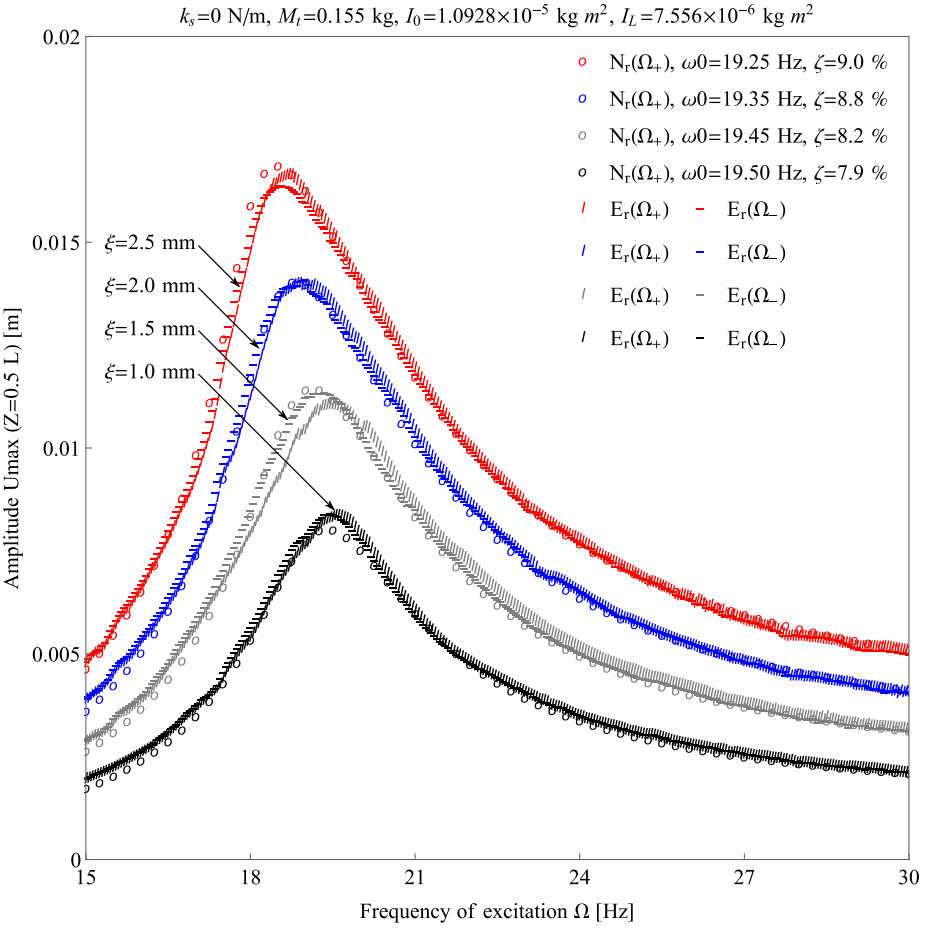

Fig. 9. Frequency response curves FEM (circles) vs. experiment (lines). Amplitude of excitation: ξ = 2.5 mm, ξ = 2 mm, ξ = 1.5 mm, ξ = 1 mm.

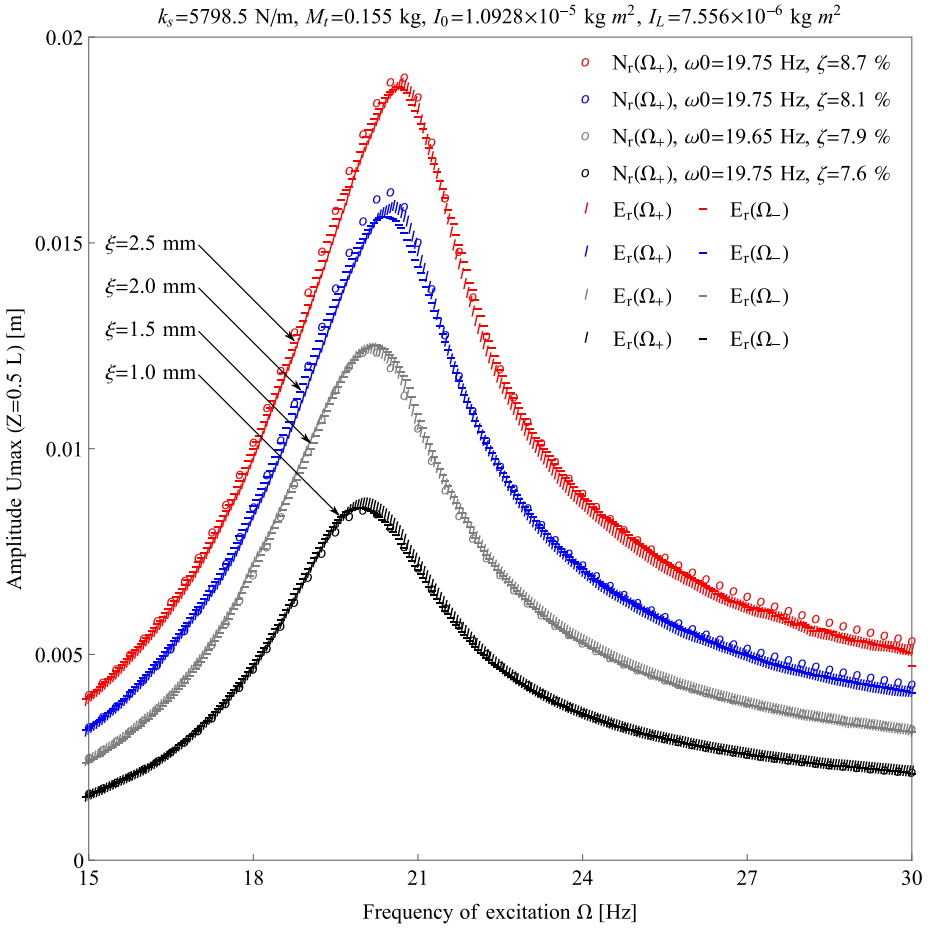

Fig. 10. Frequency response curves FEM (circles) vs. experiment (lines). Amplitude of excitation ξ = 2.5 mm, ξ = 2 mm, ξ = 1.5 mm, ξ = 1 mm.

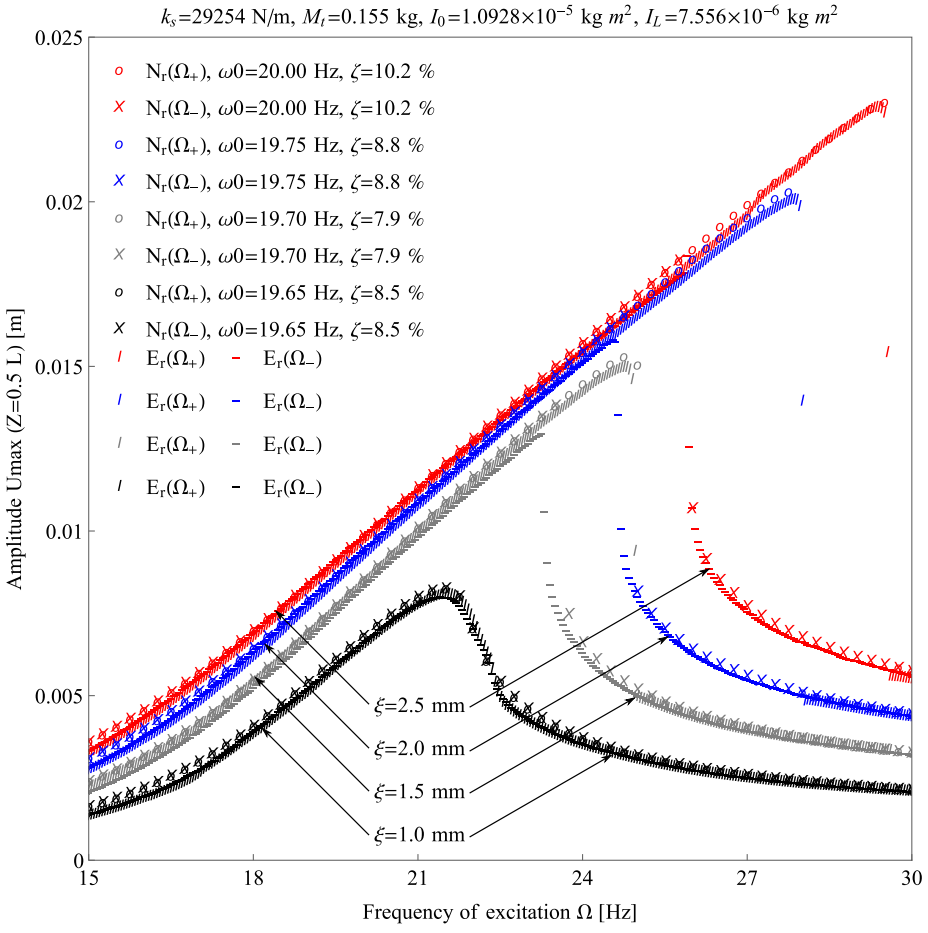

Fig. 11. Frequency response curves FEM (circles and crosses) vs. experiment (horizontal and vertical lines). Amplitude of excitation ξ = 2.5 mm, ξ = 2 mm, ξ = 1.5 mm, ξ = 1 mm.

and translation inertia of the hinges and tip mass have been taken into account as well. Four different amplitudes of excitation and three various boundary conditions in the axial direction has been considered and then numerical simulations with adjusted natural frequency (by Young modulus) and damping factor have been compared.

Previous sophisticated analytical and numerical results [16–22], which describe a smooth change from softening to hardening by increasing the stiffness of the spring, are thoroughly confirmed. Presented results (numerics vs. experiment) are in excellent agreement, much better than analytics vs. experiments shown for similar systems in [7,13,14], although in our study the beam has been excited kinematically, not parametrically. Excitation in the longitudinal direction of the system could generate another interactions.

The analysis shows that the nonlinear dynamics depends not only on boundary conditions, which of course are of great importance, but also on the environmental temperature where tests are performed. It emphasizes the importance as well as disadvantages associated with carrying out the experiment. Problems that arise in the experiment like amplitude and temperature dependent damping can have a big impact on the future work on this topic.

Declaration of Competing Interest

Stefano Lenci is a member of the Editional Board of International Journal of Mechanical Sciences. The authors declare that there are no other conflicts of interest.

Acknowledgements

This work is part of the collaboration between Polytechnic University of Marche and Lublin University of Technology, which is aimed at developing a Joined Doctoral Programme. The work is financially supported by grant 2019/33/N/ST8/02661 from the National Science Centre, Poland. Authors would like to thank MSc. Eng. Marcin Kowalczuk for his help during Young modulus and damping ratio laboratory tests.

References

[1] Timoshenko SP. X. on the transverse vibrations of bars of uniform cross-section. Lond Edinb Dublin Philos Mag J Sci 1922;43(253):125–31. doi:10.1080/14786442208633855.
[2] Atluri S. Nonlinear vibrations of a hinged beam including nonlinear inertia effects. J Mech 1973;40(1):121–6. doi:10.1115/1.3422909.
[3] Crespo da Silva MRM, Glynn CC. Nonlinear flexural-flexural-torsional dynamics of inextensional beams. i. equations of motion. J Struct Mech 1978;6(4):437–48. doi:10.1080/03601217808907348.
[4] Crespo Da Silva MRM. Non-linear flexural-flexural-torsional-extensional dynamics of beams—I. Formulation. Int J Solids Struct 1988;24(12):1225–34. doi:10.1016/0020-7683(88)90087-X.
[5] Labuschagne A, van Rensburg NFJ, van der Merwe AJ. Comparison of linear beam theories. Math Comput Model 2009;49(1–2):20–30. doi:10.1016/j.mcm.2008.06.006.
[6] Babilio E, Lenci S. On the notion of curvature and its mechanical meaning in a geometrically exact plane beam theory. Int J Mech Sci 2017;128–129:277–93. doi:10.1016/j.ijmecsci.2017.03.031.
[7] Araumi N, Yabuno H. Cubic–quintic nonlinear parametric resonance of a simply supported beam. Nonlinear Dyn 2017;90(1):549–60. doi:10.1007/s11071-017-3680-1.
[8] Lacarbonara W, Arafat HN, Nayfeh AH. Non-linear interactions in imperfect beams at veering. Int J Non Linear Mech 2005;40(7):987–1003. doi:10.1016/j.ijnonlinmec.2004.10.006.
[9] Boyaci H. Vibrations of stretched damped beams under non-ideal boundary conditions. Sadhana 2006;31(1):1–8. doi:10.1007/BF02703795.
[10] Xu Y-p, Zhou D, Cheung YK. Elasticity solution of clamped-simply supported beams with variable thickness. Appl Math Mech 2008;29(3):279–90. doi:10.1007/s10483-008-0301-1.
[11] Plat H, Bucher I. Optimizing parametric oscillators with tunable boundary conditions. J Sound Vib 2013;332(3):487–93. doi:10.1016/j.jsv.2012.09.017.
[12] Luongo A, Rega G, Vestroni F. On nonlinear dynamics of planar shear indeformable beams. J Appl Mech 1986;53(3):619–24. doi:10.1115/1.3171821.
[13] Lacarbonara W, Yabuno H. Refined models of elastic beams undergoing large in-plane motions: theory and experiment. Int J Solids Struct 2006;43(17):5066–84. doi:10.1016/j.ijsolstr.2005.07.018.
[14] Shibata A, Ohishi S, Yabuno H. Passive method for controlling the nonlinear characteristics in a parametrically excited hinged-hinged beam by the addition of a linear spring. J Sound Vib 2015;350:111–22. doi:10.1016/j.jsv.2015.03.055.
[15] Lenci S, Rega G. Nonlinear free vibrations of planar elastic beams: aunified treatment of geometrical and mechanical effects. Procedia IUTAM 2016;19:35–42. doi:10.1016/j.piutam.2016.03.007.
[16] Lenci S, Clementi F, Rega G. A comprehensive analysis of hardening/softening behaviour of shearable planar beams with whatever axial boundary constraint. Meccanica 2016;51(11):2589–606. doi:10.1007/s11012-016-0374-6.
[17] Lenci S, Clementi F, Rega G. Comparing nonlinear free vibrations of timoshenko beams with mechanical or geometric curvature definition. Procedia IUTAM 2017;20:34–41. doi:10.1016/j.piutam.2017.03.006.
[18] Lenci S, Rega G. Axial-transversal coupling in the free nonlinear vibrations of timoshenko beams with arbitrary slenderness and axial boundary conditions. Proc Math Phys Eng Sci 2016;472(2190):20160057. doi:10.1098/rspa.2016.0057.
[19] Clementi F, Lenci S, Rega G. Cross-checking asymptotics and numerics in the hardening/softening behaviour of timoshenko beams with axial end spring and variable slenderness. Arch Appl Mech 2017;87(5):865–80. doi:10.1007/s00419-016-1159-z.
[20] Kloda L, Lenci S, Warminski J. Nonlinear dynamics of a planar beam–spring system: analytical and numerical approaches. Nonlinear Dyn 2018;94(3):1721–38. doi:10.1007/s11071-018-4452-2.
[21] Kloda L, Lenci S, Warminski J. Nonlinear dynamics of a planar hinged-supported beam with one end lumped mass and longitudinal elastic support. MATEC Web Conf 2018;241:01016. doi:10.1051/matecconf/201824101016.
[22] Kloda L, Lenci S, Warminski J. Nonlinear dynamics of a planar hinged-simply supported beam with one end spring: higher order resonances. In: Kovacic I, Lenci S, editors. IUTAM Symposium on Exploiting Nonlinear Dynamics for Engineering Systems. IUTAM Bookseries, 37. Cham: Springer International Publishing; 2020. p. 155–65. doi:10.1007/978-3-030-23692-2_14.
[23] Lenci S, Clementi F. Axial-transversal coupling in the nonlinear dynamics of a beam with an inclined roller. Int J Mech Sci 2018;144:490–501. doi:10.1016/j.ijmecsci.2018.06.007.
[24] H. Poincaré, Science and hypothesis, London: W. Scott.
[25] Altuglas International Arkema Group, General information and physical properties: booklet, 2019.
[26] Spinner S, Reichard TW, Tefft WE. A comparison of experimental and theoretical relations between Young's modulus and the flexural and longitudinal resonance frequencies of uniform bars. J Res Natl Bureau Stand Sect A 1960;64A(2):147–55. doi:10.6028/jres.064a.014.
[27] T. Schultheiss, Vibration Test System TV 59335/AIT-340TGT MO 48 XL: Technical Documentation: (S/N:267/10), Schalkau, 2006.
[28] Yang Z. On an extensible beam equation with nonlinear damping and source terms. J Differ Equ 2013;254(9):3903–27. doi:10.1016/j.jde.2013.02.008.
[29] Amabili M. Nonlinear damping in large-amplitude vibrations: modelling and experiments. Nonlinear Dyn 2018;93(1):5–18. doi:10.1007/s11071-017-3889-z.
[30] Eichler A, Moser J, Chaste J, Zdrojek M, Wilson-Rae I, Bachtold A. Nonlinear damping in mechanical resonators made from carbon nanotubes and graphene. Nat Nanotechnol 2011;6(6):339–42. doi:10.1038/nnano.2011.71.
[31] Abaqus 2016 documentation